Matrix-Assisted Laser Desorption / Ionization Tandem Reflectron Time-of-Flight Mass Spectrometry of Fullerenes

Marcela M. Cordero, Timothy J. Cornish,* and Robert J. Cotter*

Middle Atlantic Mass Spectrometry Laboratory, Department of Pharmacology and Molecular Sciences, The Johns Hopkins University School of Medicine, Baltimore, Maryland, USA

A tandem reflectron time-of-flight mass spectrometer developed in our laboratory provides a unique opportunity to investigate the collision-induced dissociation of fullerene ions formed by matrix-assisted laser desorption/ionization (MALDI). Specifically, this opportunity arises from the ability to utilize high energy collisional activation (normally available only on tandem sector instruments by using continuous ionization techniques) for ions formed by pulsed laser desorption, whereas most MALDI time-of-flight instruments record product ion mass spectra of ions formed by metastable or postsource decay. In this study we investigate the products of mass-selected and collisionally activated C_{60}^+ and C_{70}^+ ions by using different target gases over a range of target gas pressures. In general, heavier target gases produce more extensive fragmentation and improve the mass resolution of lower mass ionic products because a greater portion of these ions are formed by single collisions. Additionally, the tandem time-of-flight instrument utilizes a nonlinear (curved-field) reflectron in the second mass analyzer that enables high energy collision-induced dissociation spectra to be recorded without scanning or stepping the reflectron voltage. (*J Am Soc Mass Spectrom* 1996, 7, 590–597)

The discovery of buckminsterfullerene (C_{60}) in 1985 [1, 2] and its subsequent large-scale synthesis in 1990 [3] has produced a growing research field that has expanded the fullerene family [4] to include C_{70} and many other fullerene-type molecules, as well as related carbon clusters such as the buckytubes [5]. The wide range of research on these molecules [6] now includes (among others) the application of fullerenes in the development of superconductors [7], in astrophysics [8], and in biochemistry, where fullerene derivatives have been used successfully as inhibitors of HIV-1 protease [9]. Mass spectrometry was critical to the discovery of the fullerenes and continues to be important for the determination of their physical and chemical properties. Several recent reviews [10–14] describe the wide range of desorption, ionization, and mass analysis techniques that have been applied to the study of these intriguing molecules.

A variety of excitation methods, used in conjunction with mass spectrometry and tandem mass spectrometry, have revealed that fullerene ions dissociate via C_{2n} losses when formed with excess internal energy [15–20], or when collision-induced dissociation (CID) [21] has been used to induce fragmentation by high energy collisions with gaseous targets [11, 22–27]. In contrast, the surface-induced dissociation [21, 28] of fullerenes generally has resulted in negligible fragmentation [11, 29–31].

A dual-reflectron tandem (RTOF/RTOF) time-of-flight [32] mass spectrometer has been designed in our laboratory [33–36] for the CID analysis of stable molecules formed by matrix-assisted laser desorption/ionization (MALDI). This instrument uses a single-stage (constant field) reflectron in the first mass analyzer (MS1) that is followed by an electrostatic gating system for mass selection, an open collision region in which target gases are injected by a pulsed valve, and a second mass analyzer (MS2) equipped with a curved-field reflectron (CFR) [33, 37]. This reflectron provides simultaneous focusing for product ions over a wide range of mass and energy, and obviates the need to step the reflectron voltage [38]. The MALDI technique, introduced in 1988 by Tanaka et al. [39] and Karas and Hillenkamp [40], provides an intense source of intact fullerene and fullerene derivative [41, 42] ions. At the same time, high energy CID is most easily

carried out on scanning, sector mass spectrometers and generally its use is restricted to fullerene ions formed by continuous ionization techniques, such as thermal desorption/electron impact [22–27] or liquid secondary ion mass spectrometry (SIMS) [26]. Thus, the MALDI–RTOF/RTOF instrument developed in our laboratory provides a unique opportunity to carry out CID analyses of fullerene ions formed by matrix-assisted laser desorption/ionization.

Experimental

Instrumentation

A diagram of the tandem reflectron (RTOF/RTOF) time-of-flight mass spectrometer is shown in Figure 1. Two milled, square cross-section, aluminum flight-tube assemblies, capped with perforated stainless steel sheet, provide optically accurate mounting of the reflectrons at an angle of 1.5°. The reflectrons are constructed from a series of 0.020-in. brass lens elements, with 90% transmission grids on the first and last lenses. The reflectron in MS1 is a conventional, single-stage reflectron that utilizes a series of fixed 500-KΩ resistors to provide a linear increase in potential (constant retarding field) on the lens elements. The reflectron in MS2 is a curved-field reflectron, where the voltages on the lens elements are set by a series of 2-MΩ potentiometers to follow the arc of a circle (which increases the retarding field) and are optimized for focusing at the detector by using SIMION trajectory calculations as described previously [33]. These potentiometers are located inside the vacuum system between the lens elements: they are set during construction of the instrument and are not adjusted thereafter.

Ions are formed by matrix-assisted laser desorption/ionization by using a Photon Technology International (Ontario, Canada) model PL2300, 600-ps pulsed nitrogen laser tightly focused onto the probe surface by a 2.5-cm focal-length lens mounted inside the vacuum chamber. Desorbed ions are extracted from the 4-kV probe to ground through a 5-mm single-stage extraction region, transmitted through MS1, and mass-selected and focused into the collision region and
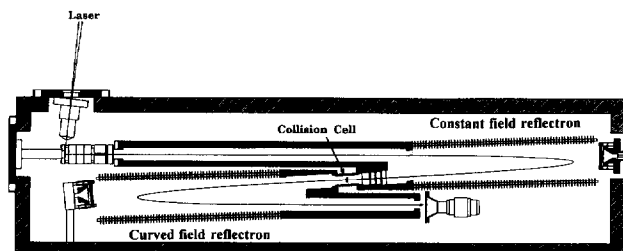

Figure 1. Schematic of the tandem reflectron (RTOF/RTOF) time-of-flight mass spectrometer with a curved-field reflectron in the second mass analyzer. Reprinted with permission from ref 33.

MS2 by a split Einzel lens–deflection system. The mass-selected ions are then dissociated by collision with target gases supplied to the collision region by a Newport (Fountain Valley, CA) model BV-100 pulsed valve. Ions were detected by using a Galileo (Sturbridge, MA) dual channel-plate detector, and mass spectra were recorded on a Tektronix (Beaverton, OR) model TDS-540, 1 × 10^9 samples per second (500 MHz bandwidth) transient recorder–digital oscilloscope downloaded onto a 486 PC and processed by using TOFWARE from ILYS Software (Pittsburgh, PA). Generally, the transients from 100–200 laser shots were signal-averaged for each mass spectrum.

Calibration

Calibration of precursor ion masses is carried out in the same manner as for single TOF instruments and standards of known molecular mass are used. In this case, bradykinin (monoisotopic MH$^+$ = 1059.94), renin substrate tetradecapeptide (1759.94), and substance P (1347.73) were used. On the other hand, product ion calibration is basically an instrument function that is described by the equation for an ellipse, whose constants are programed into TOFWARE during initial setup of the instrument (by recording the product ion mass spectrum of a compound with known fragment masses) and reprogramed only when the instrument is disassembled for modification [43].

Sample Preparation

Buckminsterfullerene (C_{60}), [5,6]-fullerene C_{70}, and the matrix compound α-cyano-4-hydroxycinnamic acid were purchased from Aldrich (Milwaukee, WI), and used without further purification. Benzene, purchased from Baker Laboratories (Phillipsburg, NJ), was used to make saturated solutions of C_{60}, C_{70}, and α-cyano-4-hydroxycinnamic acid. Ten microliters of each chemical were mixed and allowed to spread over the probe tip and dry slowly to produce visible crystals. High purity collision gases were obtained as follows: helium (99.999%) from Connecticut Gas Inc. (Stratford, CT), argon (99.999%) from Potomac Airgas Inc. (Linthicum, MD), and xenon (99.999%) and SF_6 (99.99%) from Matheson (East Rutherford, NJ).

Results and Discussion

Figure 2a shows the mass spectrum of a mixture of C_{60} and C_{70} recorded by passing the ions through both reflectrons without mass selection or introduction of the collision gas. For both of these species, prompt fragmentation (that occurs in the ion source) is observed that leads to losses of two, four, and six carbon atoms. Additionally, in this double-reflectron mode mass resolution [full width at half maximum (FWHM)] was approximately 2000 for C_{60}^+ and C_{70}^+, as observed
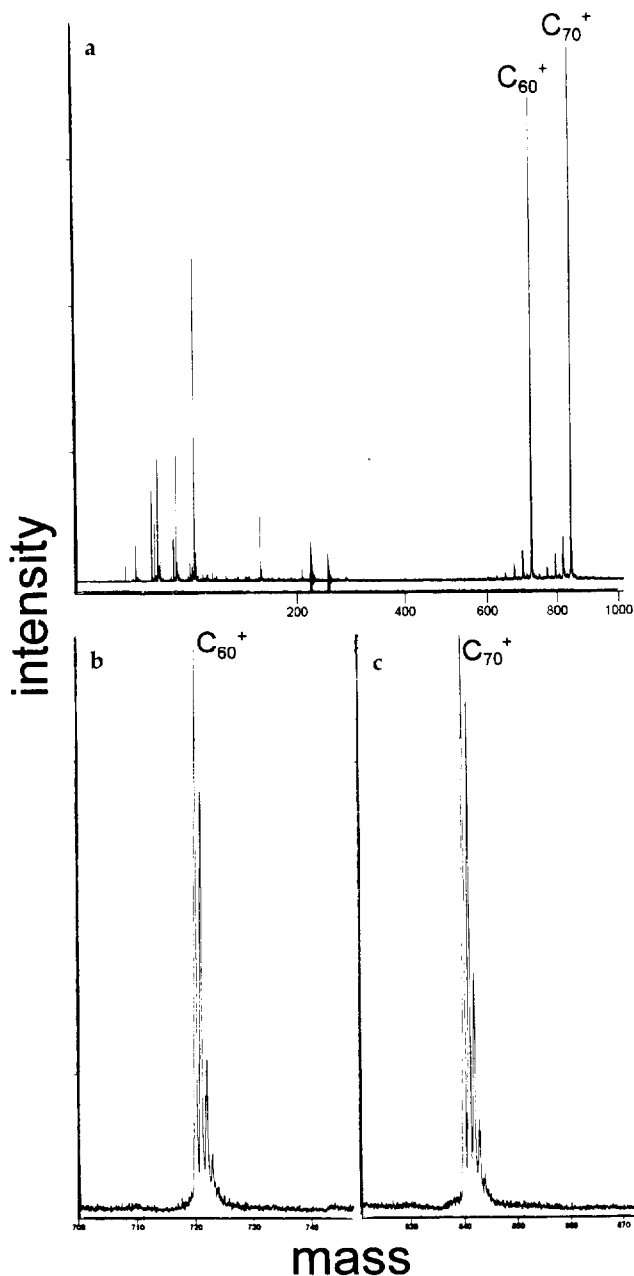
Figure 2. (a) Mass spectrum of a mixture of C_{60} and C_{70} obtained by passing the beam through both reflectron mass analyzers. Molecular ion regions for (b) C_{60}^+ and (c) C_{70}^+.

Figure 3. Mass selection of (a) C_{60}^+ and (b) C_{70}^+ by using a deflection gating system placed just ahead of the collision region.

in the expanded mass spectra shown in Figure 2b and c, respectively. Mass selection of C_{60}^+ and C_{70}^- ions is shown in Figure 3a and b, respectively. The mass spectra in Figure 3 also record a signal from the ion gating pulse, which (because it is located at the entrance to the collision region between the two mass analyzers) appears at about one half the flight time of the ion selected. Figure 3 illustrates the fact that the mass resolution of molecular ions, in the absence of a collision gas, is unaffected by the mass gating system.
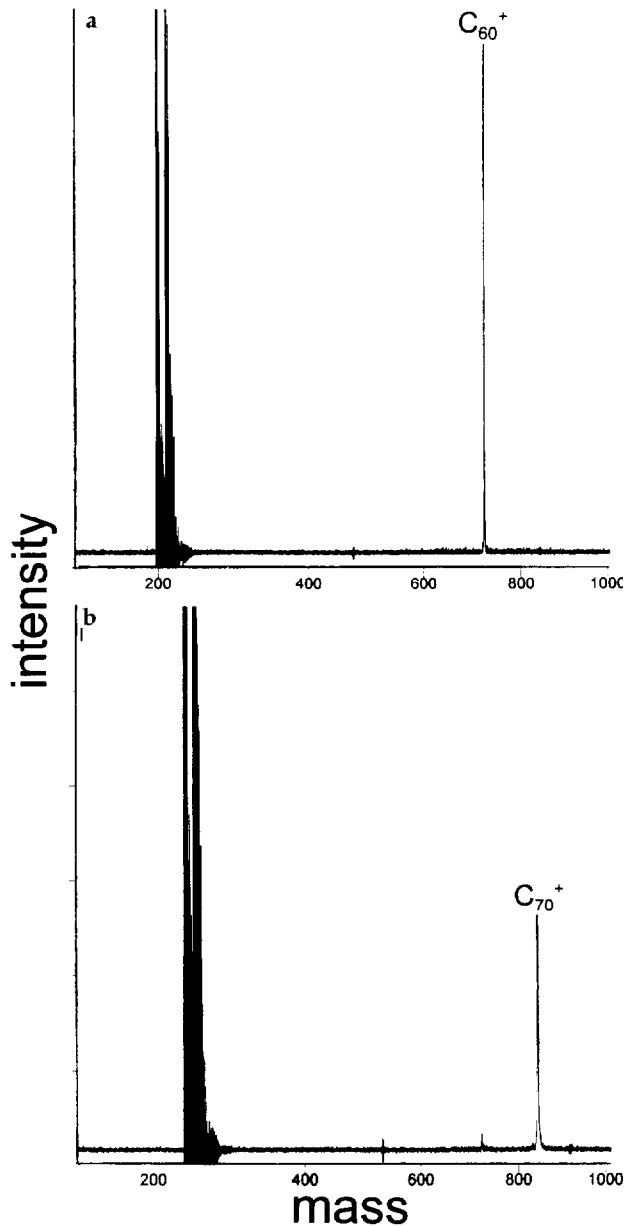
Collision-Induced Dissociation of C_{60}

By using helium, argon, and xenon as collision gases, CID mass spectra were obtained separately from C_{60} and C_{70} samples (rather than mixtures of the two fullerenes); however, mass selection (gating) was used to eliminate contributions to the spectrum from prompt fragmentation. The pulsed valve used in this instrument for collision-induced dissociation produces a 100–200-μs (FWHM) pulse of the target gas, whose maximum (instantaneous) pressure is not determined easily, but is controlled by the gas pressure at the inlet to the valve. In our first experiment, we utilized helium pressures that resulted in low (20%), medium (80%), and high (100%) attenuation of C_{60}. In subse-

quent experiments (for both C_{60} and C_{70}), similar inlet pressures were used for argon and xenon.

Figure 4 shows CID mass spectra of mass-selected C_{60}^{+} ions at low, medium, and high attenuation by using helium gas. The series of C_{2n}^{+} peaks observed at low attenuation (Figure 4a) is more fully developed at medium attenuation (Figure 4b), which favors clusters C_{44}^{+} and C_{50}^{+} as reported previously for CID mass spectra [22–27]. The threshold for this series of C_{2n}^{+} ions at C_{30}^{+}/C_{32}^{+} is maintained in the high attenuation product ion mass spectrum (Figure 4c), which also reveals a poorly resolved, low mass C_{n}^{+} series. Previous studies that involved the reionization of neutral dissociation products shows that C_{60}^{+} fragments by loss of large C_{2n} neutrals rather than by stepwise C_2 losses [27]. For singly charged C_{60} molecules, the largest detectible neutral loss was C_{28}, the neutral complement of C_{32}^{+}, which is consistent with the increase in the ratio of C_{32}^{+} to C_{30}^{+} observed (Figure 4c) in the distribution of product ions formed at higher attenuation.

Collision-induced dissociation of C_{60}^{+} by argon (Figure 5) results almost exclusively in the production of low mass C_{n}^{-} ions. The product ion distribution observed in Figure 5b, in which peaks that correspond to C_{11}^{+}, C_{15}^{+}, C_{19}^{+} and C_{23}^{+} have higher abundances, is similar to that reported for the laser ablation of graphite [44–47], and results from catastrophic collisions [23]. In addition, these C_{n}^{+} species are resolved considerably better than the species shown in Figure 4c. It is likely that these lower mass fragments are formed only when there is considerably more collisional energy available than required for the formation of the higher mass C_{2n}^{+} ions. For C_{60}^{+} ions with translational energies of 4 keV, the relative energy (E_{cm} in the center-of-mass frame) is only 22 eV for collisions with helium and 210 eV for argon [21]. Thus, it is likely that the C_{n}^{+} ions shown in Figure 5b are formed largely by single collisions with argon, whereas the less resolved low mass spectrum shown in Figure 4c reflects the need for multiple collisions with helium to provide sufficient activation for the formation of C_{n}^{+} ions. This theory is consistent with the fact that high attenuation with argon (Figure 5c) favors the formation of lower mass C_{n}^{+} species, but results in loss of mass resolution.

Formation of low mass C_{n}^{+} ions is observed even at low attenuation pressures of xenon (Figure 6a), where the relative translational energy available for activation is 616 eV. However, at high attenuation (Figure 6c) there was considerable reduction in the fragmentation observed, most likely the result of loss of ions from scattering with this heavier gas. Product ion mass spectra that result from collision-induced dissociation with SF_6 also were obtained (data not shown). Although the collision energy is also high in this case (674 eV), poor signal-to-noise ratio was observed for product ions, which most likely results from high scattering losses when this target gas is used.
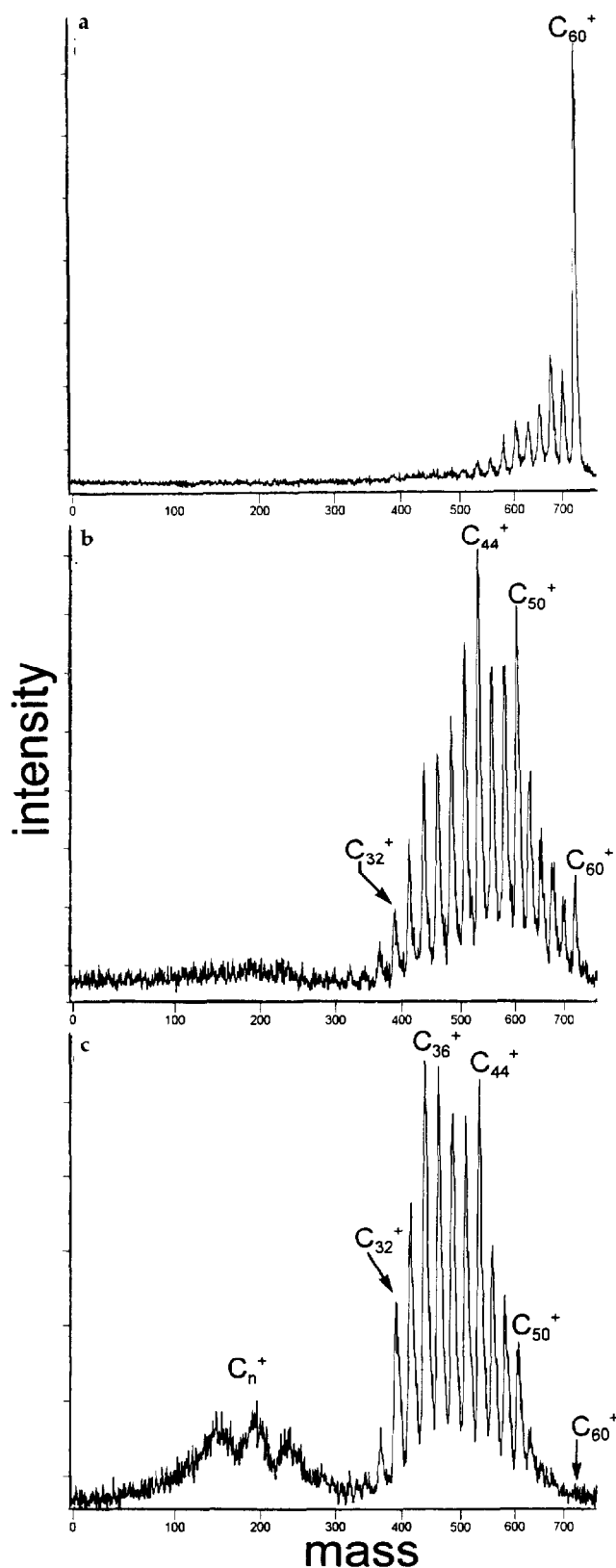

Figure 4. Collision-induced dissociation of C_{60}^{+} by using helium as the target gas at (a) low, (b) medium, and (c) high attenuation as described in the text.
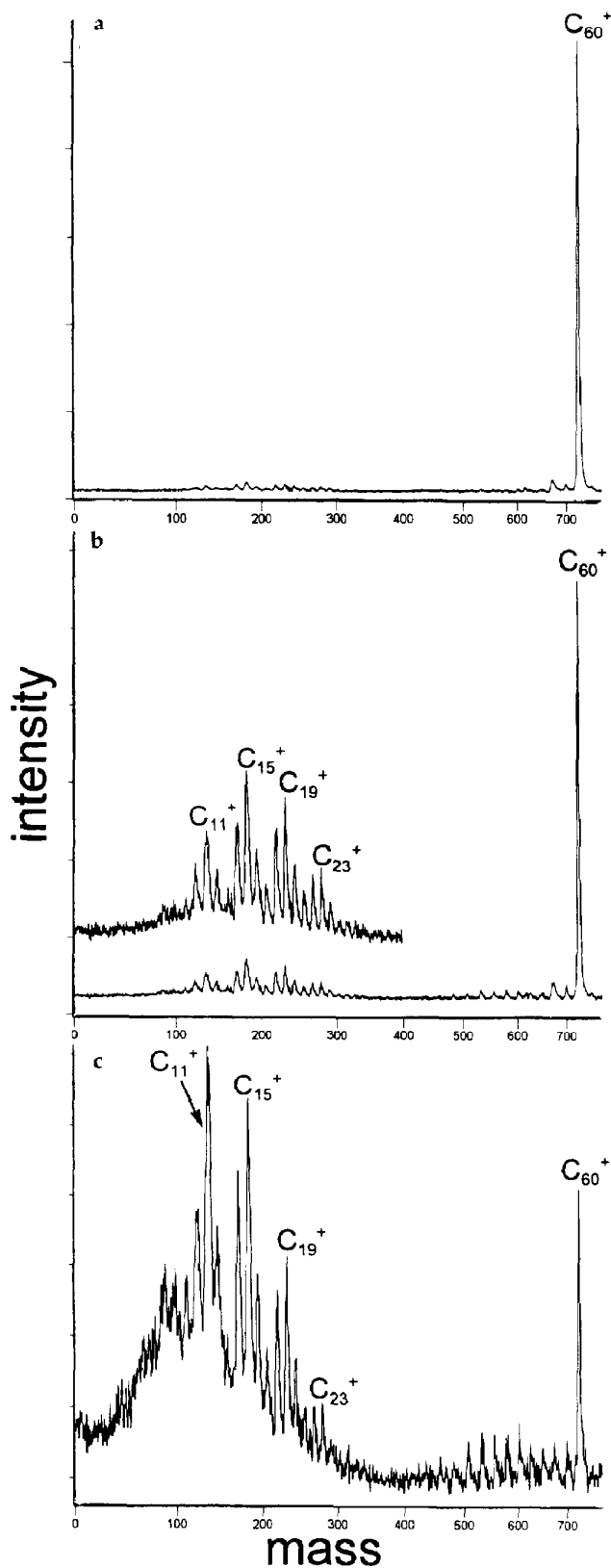
Figure 5. Collision-induced dissociation of C_{60}^+ by using argon as the target gas at (a) low, (b) medium, and (c) high attenuation as described in the text.
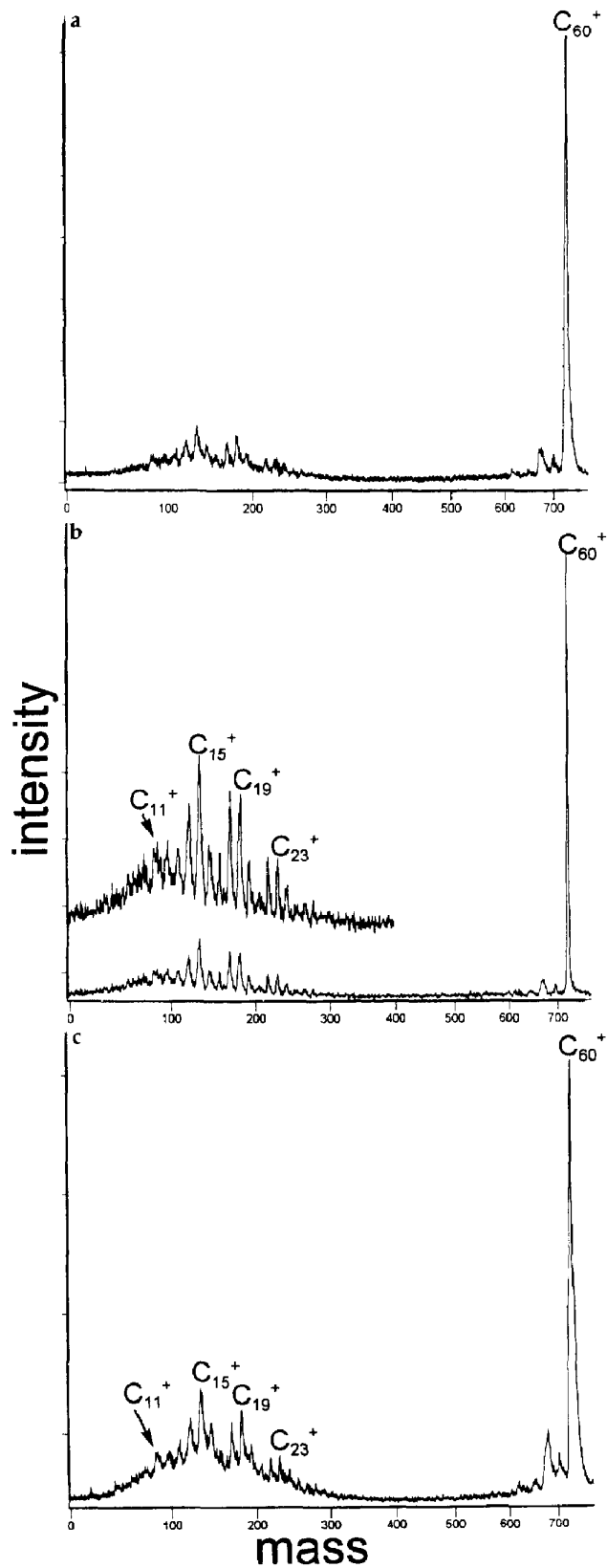
Figure 6. Collision-induced dissociation of C_{60}^+ by using xenon as the target gas at (a) low, (b) medium, and (c) high attenuation as described in the text.

Collision-Induced Dissociation of C_{70}

Very similar results were observed for the collision-induced dissociation mass spectra of C_{70}^+. At low attenuation by helium (Figure 7a) successive C_2 losses are observed, whereas the major fragment ion formed is C_{60}^+. At medium (Figure 7b) and high (Figure 7c) attenuation, the fragmentation pattern resembles that for C_{60}^+, which favors formation of C_{44}^+, C_{50}^+ and C_{56}^+ ions. At high attenuation, an unresolved signal that corresponds to low mass C_n^+ ions is observed. Collisions of C_{70}^+ with argon result predominantly in the production of the same low mass C_n^+ ions observed for C_{60}^+ (Figure 8), but require considerably higher attenuation. As before, higher intensities were observed for the odd carbon clusters C_{11}^+, C_{15}^-, C_{19}^+, and C_{23}^+ (Figure 8b). These low mass ions were also observed by using xenon and SF_6 as collision gases (data not shown); *again*, the spectra obtained showed considerably less ion signal intensity due to losses from ion scattering.

Conclusions

As would be expected, the most efficient and informative fragmentation and the best resolved collision-induced dissociation spectra were recorded under conditions that promote fragmentation from single collisions. For C_{60}^+ these correspond to the spectra shown in Figures 4b and 5b, in which medium attenuation (approximately 80%) by helium and argon results in efficient activation of C_{60}^+ to form high mass C_{2n}^+ and low mass C_n^+ ions, respectively. In this respect, the tandem reflectron (RTOF/RTOF) instrument is analogous to multiple sector mass spectrometers that use high energy collision-induced dissociation. This (in fact) has been the intent in its design, in which we elected to utilize pulsed introduction of a collision gas, rather than laser-induced photodissociation or surface-induced dissociation. In so doing, it has been possible to utilize the high fragmentation efficiency of collision-induced dissociation (normally limited to continuous ionization techniques on sector instruments) for ions formed by pulsed laser ionization.

Heavier target gases (argon, xenon, and SF_6) were utilized to provide higher collision energies (in the center-of-mass frame) in a tandem instrument designed to produce ions with relatively low (4-keV) translational energies. Similar results also might have been produced by using higher ion kinetic energies with helium as the collision gas. Formation of endohedral complexes with He and other gases has been observed over a range of translational energies [24–26, 48]. Although such complexes have been detected at laboratory energies comparable to our own [26], their resolution in the product ion mass spectra is difficult, because the gating system currently admits the entire isotopic distribution of molecular ion masses. At the same time, the current instrument has provided a
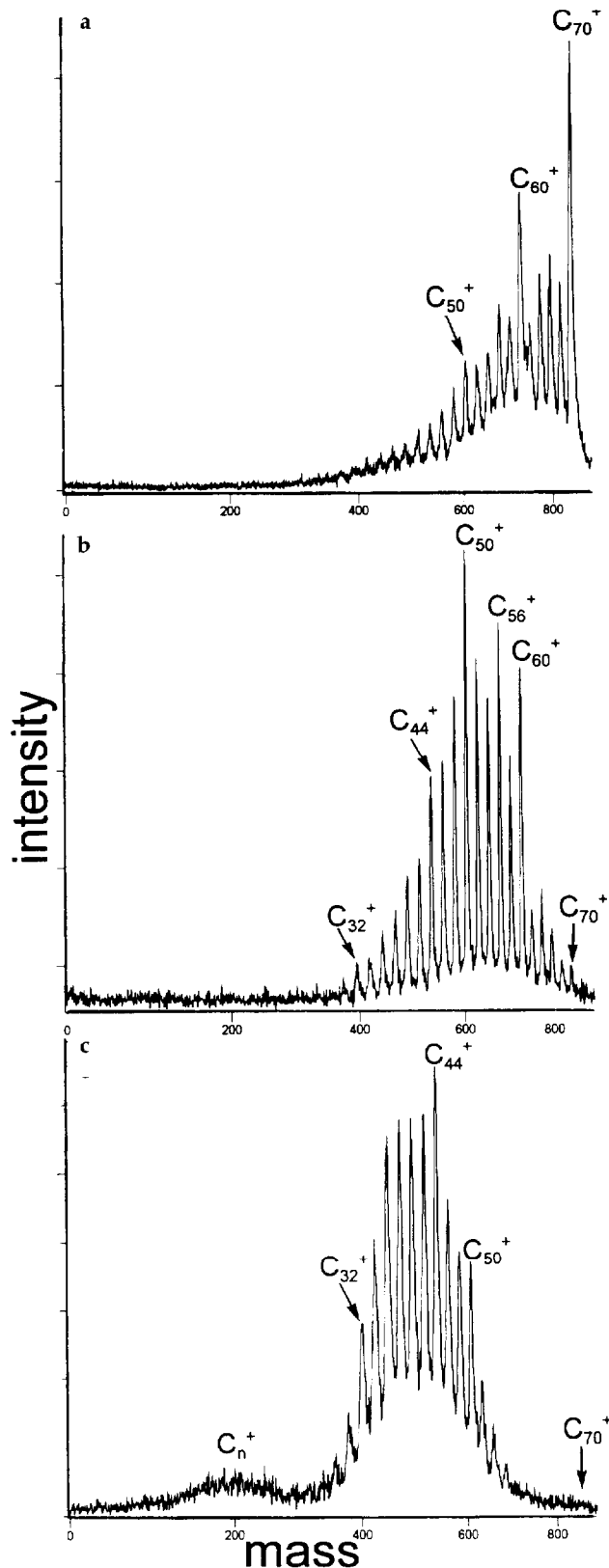

Figure 7. Collision-induced dissociation of C_{70}^+ by using helium as the target gas at (a) low, (b) medium, and (c) high attenuation as described in the text.
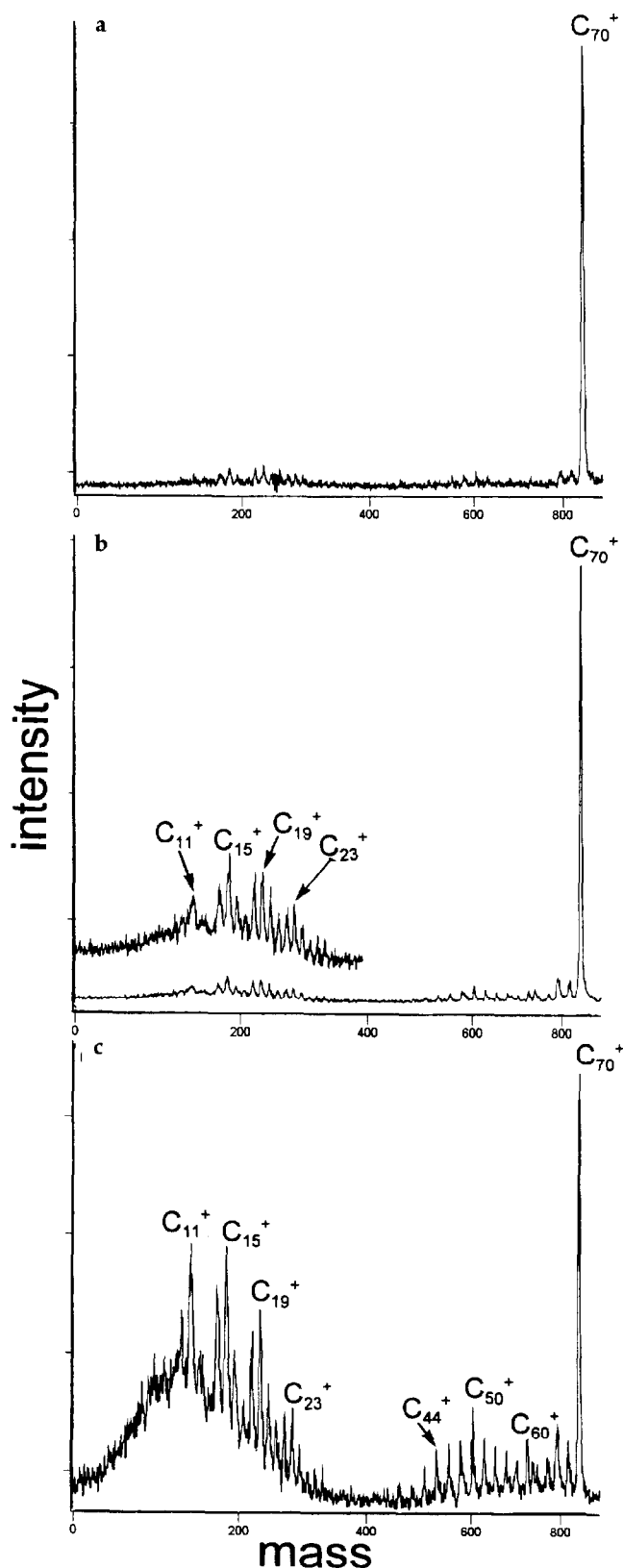
Figure 8. Collision-induced dissociation of C_{70}^- using argon as the target gas at (a) low, (b) medium, and (c) high attenuation as described in the text.

unique opportunity to compare such CID results for fullerene ions formed by MALDI on a unique tandem time-of-flight mass spectrometer with those formed by other methods on sector mass spectrometers.

Acknowledgments

References

1. Kroto, H. W.; Heath, J. R.; O'Brien, S. C.; Curl, R. F.; Smalley, R. E. Nature (London) 1985, 318, 162–163.
2. Rohlting, E. A.; Cox, D. M.; Kaldor, A. J. Chem. Phys. 1984, 81, 3322–3330.
3. Krätschmer, W.; Lamb, L. D.; Fostiropoulos, K.; Huffman, D. R. Nature (London) 1990, 347, 354–358.
4. Kroto, H. Pure Appl. Chem. 1990, 62, 407–415.
5. Iijima, S. Nature (London) 1991, 354, 56–58.
6. Curl, R. F.; Smalley, R. E. Scientific American 1991, 33, 54–63.
7. Diederich, F.; Whetten, R. L. Angew. Chem. Int. Ed. Engl. 1991, 30, 678–680.
8. Kroto, H. Science 1988, 242, 1139–1145.
9. Friedman, S. H.; DeCamp, D. L.; Sijbesma, R. P.; Srdanov, G.; Wudl, F.; Kenyon, G. L. J. Am. Chem. Soc. 1993, 115, 6506–6509.
10. Greenwood, P. F. Org. Mass Spectrom. 1994, 29, 61–77.
11. Lifschitz, C. Mass Spectrom. Rev. 1993, 12, 261–284.
12. Schwarz, H. Angew. Chem. Int. Ed. Engl. 1993, 32, 1412–1415.
13. McElvany, S. W.; Ross, M. M.; Callahan, J. H. Acc. Chem. Res. 1992, 25, 162–168.
14. McElvany, S. W.; Ross, M. M. J. Am. Soc. Mass Spectrom. 1992, 3, 268–280.
15. O'Brien, S. C.; Heath, J. R.; Curl, R. F.; Smalley, R. E. J. Chem. Phys. 1988, 88, 220–230.
16. Weiss, F. D.; Elkind, J. L.; O'Brien, S. C.; Curl, R. F.; Smalley, R. E. J. Am. Chem. Soc. 1988, 110, 4464–4465.
17. Radi, P. P.; Hsu, M. T.; Brodbelt-Lustig, J.; Rincon, M.; Bowers, M. T. J. Chem. Phys. 1990, 92, 4817–4821.
18. Luffer, D. R.; Schram, K. H. Rapid Commun. Mass Spectrom. 1990, 4, 552–556.
19. Wurz, P.; Lykke, K. R. J. Phys. Chem. 1992, 96, 10129–10139.
20. Takayama, M.; Shinohara, H. Int. J. Mass Spectrom. Ion Processes 1993, 123, R7–R11.
21. Busch, K. L.; Glish, G. L.; McLuckey, S. Mass Spectrometry/Mass Spectrometry; VCH Publishers: New York, 1988.
22. Young, A. B.; Cousins, L. M.; Harrison, A. G. Rapid Commun. Mass Spectrom. 1991, 5, 226–229.
23. Doyle, R. J., Jr.; Ross, M. M. J. Phys. Chem. 1991, 95, 4954–4956.
24. Ross, M. M.; Callahan, J. H. J. Phys. Chem. 1991, 95, 5270–5273.
25. Weiske, T.; Böhme, D. K.; Hrušák, J.; Krätschmer, W.; Schwarz, H. Angew. Chem. Int. Ed. Engl. 1991, 30, 884–886.
26. Caldwell, K. A.; Giblin, D. E.; Gross, M. L. J. Am. Chem. Soc. 1992, 114, 3743–3756.
27. McHale, K. J.; Polce, M. J.; Wesdemiotis, C. J. Mass Spectrom. 1995, 30, 33–38.
28. Cooks, R. G.; Ast, T.; Mabud, Md. A. Int. J. Mass Spectrom. Ion Processes 1990, 100, 209–265.

29. Beck, R. D.; St. John, P.; Alvarez, M. M.; Diederich, F.; Whetten, R. L. *J. Chem. Phys.* **1991**, *95*, 8402–8409.

30. McElvany, S. W.; Ross, M. M.; Callahan, J. H. *Proc. Mater. Res. Soc. Symp.* **1991**, *206*, 697–702.

31. Callahan, J. H.; Somogyi, A.; Wysocki, V. H. *Rapid Commun. Mass Spectrom.* **1993**, *7*, 693–699.

32. Cornish, T. J.; Cotter, R. J. In *Time-of-Flight Mass Spectrometry*; Cotter, R. J., Ed.; American Chemical Society: Washington, DC, 1994; pp. 95–107.

33. Cornish, T. J.; Cotter, R. J. *Rapid Commun. Mass Spectrom.* **1993**, *7*, 1037–1040.

34. Cornish, T. J.; Cotter, R. J. *Org. Mass Spectrom.* **1993**, *28*, 1129–1134.

35. Cornish, T. J.; Cotter, R. J. *Anal. Chem.* **1993**, *65*, 1043–1047.

36. Cornish, T. J.; Cotter, R. J. *Rapid Commun. Mass Spectrom.* **1992**, *6*, 242–248.

37. Cornish, T. J.; Cotter, R. J. *Rapid Commun. Mass Spectrom.* **1994**, *8*, 781–785.

38. Kaufmann, R.; Kirsch, D.; Spengler, B. *Int. J. Mass Spectrom. Ion Processes* **1994**, *131*, 355–385.

39. Tanaka, K.; Waki, H.; Ido, Y.; Akita, S.; Yoshida, Y.; Yoshida, T. *Rapid Commun. Mass Spectrom.* **1988**, *2*, 151–153.

40. Karas, M.; Hillenkamp, F. *Anal. Chem.* **1988**, *60*, 2299–2301.

41. Sijbesma, R.; Srdanov, G.; Wudl, F.; Castoro, J. A.; Wilkins, C.; Friedman, S. H.; DeCamp, D. L.; Kenyon, G. L. *J. Am. Chem. Soc.* **1993**, *115*, 6510–6512.

42. Yao, J.; Castoro, J. A.; Wilkins, C. L.; An, Y.-Z.; Rubin, Y. *Proceedings of the 42nd ASMS Conference on Mass Spectrometry and Allied Topics*; Chicago, IL, 1994; p 589.

43. Cordero, M. M.; Cornish, T. J.; Cotter, R. J. *Rapid Commun. Mass Spectrom.* **1995**, *9*, 1356–1361.

44. Bloomfield, L. A.; Geusic, M. E.; Freeman, R. R.; Brown, W. L. *Chem. Phys. Lett.* **1985**, *121*, 33–37.

45. Heath, J. R.; O'Brien, S. C.; Zhang, Q.; Liu, Y.; Curl, R.F.; Kroto, H. W.; Tittel, F. K.; Smalley, R. E. *J. Am. Chem. Soc.* **1985**, *107*, 7779–7780.

46. O'Keefe, A.; Ross, M. M.; Baronavski, P. *Chem. Phys. Lett.* **1986**, *130*, 17–19.

47. McElvany, S. W.; Creasy, W. R.; O'Keefe, A. *J. Chem. Phys.* **1986**, *85*, 632–633.

48. Schwarz, H.; Weiske, T.; Bohme, D. K.; Hrusak, J. In *Buckminsterfullerenes*; Billups, W. E.; Ciufolini, M. A., Eds.; VCH Publishers: New York, 1993; p 257 and references therein.